Self-assembled polypyrrole film by interfacial polymerization for supercapacitor applications

Qinghao Yang, Zhenzhong Hou, Tianzhu Huang

College of Material Science and Engineering, Xi'an University of Science and Technology, Xi'an 710054, People's Republic of China
Correspondence to: Z. Hou (E-mail: hzzhong1981@yeah.net)

ABSTRACT: A facile interfacial synthesis strategy is proposed to synthesize self-assembled polypyrrole (PPy) free-standing films for electrochemical capacitors with the assistance of surfactants. The chemical structure of the obtained samples is characterized by Fourier transform infrared. The morphologies of the samples are studied by scanning electron microscope. The results show that the prepared PPy films own highly porous structures using Tween80 as a surfactant, while the synthesized PPy films have vesicular structures by adding Span80 as a surfactant. Furthermore, lowering polymerization temperature makes PPy films have smaller and more pores or vesicles. The PPy films prepared at $0°C$ with Tween80 as a surfactant possess a high specific capacitance of 261 F g^{-1} at 25 mV s^{-1} as well as retain 75% of the initial specific capacitance value after 1000 cycles. The good electrochemical properties can be attributed to the highly porous structural advantage of the PPy films caused by Tween80. © 2014 Wiley Periodicals, Inc. J. Appl. Polym. Sci. **2015**, *132*, 41615.

INTRODUCTION

Novel materials for energy storage device are the basis for the development in clean renewable energy area. One of the most exciting recent developments in this field is the use of conducting polymers, especially polypyrrole (PPy), as electrode material for supercapacitors. Among the conducting polymers, PPy is particularly promising, because of its high and adjustable conductivity, environmental stability, and relatively ease to synthesize.[1–5] It has found use in a wide range of applications, including chemical and biological sensors,[6] actuators,[7] light-emitting diodes,[8] corrosion resistance,[9] advanced battery systems,[10] and electrochemical supercapacitors.[11] In the field of supercapacitors, PPy is especially applicable for the active material due to its good reversible doping–dedoping property, low toxicity, facile preparation, and steady performance. As is known to all, PPy can be directly synthesized by both chemical and electrochemical processes. However, electrochemical storage requires large weight of active materials, so the chemical synthesis is more appropriate than the electrochemical way. So far, the supercapacitors based on pure PPy active material generally show the specific capacitance of 200–400 F g^{-1}.[12,13] Therefore, it is still a challenge to improve the capacitance of PPy-based supercapacitors for the needs of high performance in the new energy field.

It is well known that the microstructure and the morphology of the active material have a significant influence on the charge storage properties. So preparing the active material with micro/nanostructures is one of the available methods to improve its supercapacitor properties.[14] Recently, Tran-Van and coworkers reported the effect of morphological parameters, like particle size and specific surface area, on the electrochemical storage properties.[15] A classical chemical way of interfacial polymerization is usually used to control the morphology of the conducting polymer. Since the polymerization occurs primarily at the interface between the aqueous and organic phases, the so-called "secondary growth" phenomenon can be effectively suppressed, leading to the polymer with special micro/nanostructures instead of the bulk product.[16–18] Dallas *et al.* synthesized submicron PPy with the mean diameter of 200–300 nm and silver/PPy nanocomposites by an interfacial polymerization in the interface of water/chloroform mixture.[19] Dolui and coworker have prepared irregular sphere-like PPy microparticles and PPy/graphene oxide nanocomposites at the interface between water and chloroform.[20] Liu *et al.* fabricated PPy hollow microspheres with size in the range of 1.7–2.2 μm via interfacial polymerization in the presence of sodium dodecyl benzene sulfonate.[21] The obtained PPy hollow microspheres show the specific capacitances of 146.4 F g^{-1}, which is potential materials for supercapacitors. Recently, a novel ternary phase interfacial synthesis

Table I. Experimental Parameters and Conditions of the Obtained PPy Samples

Samples	Py (mol)	FeCl$_3$ (mol)	APS (mol)	Tween80 (g L^{-1})	Span80 (g L^{-1})	Reaction temperature (°C)
R1	0.02	0	0.03	0	0	25
R2	0.02	0	0.03	0	0	0
R3	0.02	0.03	0	0	0	25
R4	0.02	0.03	0	0	0	0
R5	0.02	0.03	0	2	0	25
R6	0.02	0.03	0	2	0	0
R7	0.02	0.03	0	0	2	25
R8	0.02	0.03	0	0	2	0

strategy has been proposed to PPy samples for electrochemical capacitors. Yuan and coworkers prepared coral-like PPy by water/ionic liquid/chloroform three-phase interface route.[22] In this work, ionic liquid as intermediate phase played an important role of "buffering zone" to control the PPy polymerization process. The synthesized PPy by the three-phase strategy possessed better conductivity and less charge transfer resistance, larger specific capacitance, and improved electrochemical stability than PPy prepared by the traditional two-phase route. Han et al.[23] have synthesized core–shell structured PPy/carbon nanotubes nanocomposites through the ternary phase interfacial polymerization with ionic liquid, water, and organic phases from bottom to top. The obtained nanocomposites exhibited the high specific capacitance of 228 F g^{-1} as well as an ideal capacitor-like behavior.

Here facile water/organic two-phase interface route was used to synthesize self-assembled PPy free-standing film with three-dimensional network structures in the presence of long-chain surfactants of Tween80 or Span80. The optimized PPy film displayed improved electrochemical capacitance in 1M NaNO$_3$ aqueous solution. The effects of polymerization temperature, polymerization time, and surfactant on the structure and morphology, and pseudocapacitance of as-prepared PPy films were also investigated.

EXPERIMENTAL

Materials

Pyrrole (Py) monomer was purchased from Shannxi Chemical Reagent Co. Ltd and distilled under reduced pressure before use. Ferric chloride (FeCl$_3$) and ammonium persulfate (APS) as oxidants were obtained from Tianjin BASF chemical. Tween80 and Span80 (Tianjin Chenfu Chemical Reagent Company, China) as surfactants, and p-toluenesulfonic acid as a dopant (Shannxi Chemical Reagent Co. Ltd, China) were used as received. Apart from Py monomer, all the reagents were of analytical grade and used as supplied without further purification.

Characterization

Fourier transform infrared (FTIR) spectra were recorded on a Bruker FTIR Equinox 55 spectrophotometer using KBr pellets. The morphologies of PPy samples were observed by a scanning electron microscope (SEM; JSM6460LV, Japanese electronics, Japan). The electrical conductivity of PPy films with

the thickness of 5–8 μm was examined by a four-point probe method at room temperature with a SDY-4 digital four-probe meter made in China. Cyclic voltammetry (CV) measurements were performed in a potential range from 0.0 to 0.6 V, and a sweep rate of 25 mV s^{-1} with CS 350 electrochemical workstation (Corrtest Corporation, Wuhan, China) at room temperature. All electrochemical experiments were carried out in 1M NaNO$_3$ aqueous solution using a three-electrode system, which contained a saturated calomel electrode (SCE) and a platinum plate (ca. 1 cm^2) as the reference electrode and counter electrode, respectively; the obtained PPy films (ca. 1 cm^2) adhered on the pretreated glass carbon by Nafion (5% solution, DuPont) as the working electrode.

The specific capacitance can be calculated by the following equation from CV curves:[24,25]

$$C = \int \frac{I}{vmV} dV \qquad (1)$$

where C, I, m, v, and V are the specific capacitance (F g^{-1}), the response current (A), the mass of the electroactive material in the electrode (g), the potential scan rate (V s^{-1}), and the potential (V), respectively.
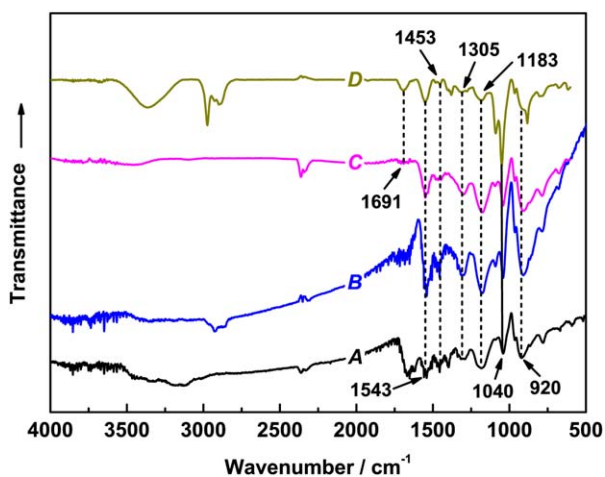
Synthesis

PPy free-standing films were synthesized through oil/water interfacial polymerization with the assistance of surfactants. The typical route is as follows: appropriate Py was dissolved in 100 mL chloroform to form the oil phase (organic phase), and a certain amount of oxidant and surfactant were dissolved in 100 mL deionized water, which was named as the water phase. Then the water phase was added to the oil phase rapidly in a 300-mL beaker at 25°C or 0°C, and the polymerization occurred on the oil/water interface. After 8 h, the as-prepared products were collected by filtration and washed with deionized water and ethanol for several times until the filtrate became colorless. Finally, the obtained black polymer free-standing films were dried at 60°C for 12 h in a vacuum oven. Detailed experimental parameters and conditions for every PPy sample are listed in Table I.

RESULTS AND DISCUSSION

Structure Characterization

The FTIR spectra of synthesized PPy films at different conditions are illustrated in Figure 1, respectively. It can be seen, from this

Figure 1. FTIR spectra of PPy films synthesized by interfacial polymerization at different conditions: (A) with $FeCl_3$ as oxidant; (B) with APS as oxidant; (C) with $FeCl_3$ as oxidant and Tween80 as surfactant; (D) with $FeCl_3$ as oxidant and Span80 as surfactant. [Color figure can be viewed in the online issue, which is available at wileyonlinelibrary.com.]

figure, that the four spectra of PPy films exhibit similar characteristic absorptions, indicating that their similar molecular structures. The broad band between 3000 and 3500 cm^{-1} corresponds to the N—H stretching of Py units in polymers. The two peaks at 1543 cm^{-1} and 1453 cm^{-1} can be attributed to the asymmetric and symmetric stretching vibrations of Py rings, respectively.[26] The band at about 1305 cm^{-1} is ascribed to the C—N stretching in Py rings of the PPy backbones.[27] The obvious peak at 1183 cm^{-1} reflect the C—H stretching of Py rings, while the peaks of C—H deformation vibrations appear at 1040 cm^{-1} and 920

cm^{-1}, which correspond to C—H in-plane deformation and C—H out-of-plane deformation, respectively.[28] The weak band at 1691 cm^{-1} is only observed in the PPy synthesized with an assistance of Tween80 or Span80 (spectra C and D in Figure 1), which is assigned to C=O characteristic absorption, revealing a small amount of residual surfactant in PPy. Though synthesized PPy has similar molecular structures, PPy films with APS as oxidant are more fragile and show worse self-assembly behaviors during the synthesis.

Morphology Characterization

Figure 2 shows the SEM images of PPy films synthesized with/without surfactants at 25°C and 0°C. In the absence of surfactant, the obtained PPy film exhibits a fine particles aggregated morphology with particle size of about 500 nm [Figure 2(a)]. Since polymerization is confined to the oil/water interface, the overgrowth of polymer can be effectively suppressed,[16] resulting in small PPy particles rather than bulk one by conventional solution polymerization. When adding Tween80, the prepared PPy film shows irregularly porous structure [Figure 2(b,c)]. Comparing these two figures, it can be seen Tween80 assists the formation of porous structure and the polymerization temperature affect the pore size significantly. Obviously, the pore size of PPy film obtained at 0°C is much smaller than that of PPy film synthesized at 25°C. When adding Span80, the prepared PPy film exhibits vesicular structure with ruptured vesicles gathered together and the PPy film produced at 0°C displays more and smaller vesicles [Figure 2(d,e)]. The influence of polymerization temperature on the morphology of PPy films can be attributed to lower temperature decreasing surfactant micelle size as well as reducing polymerization rate.
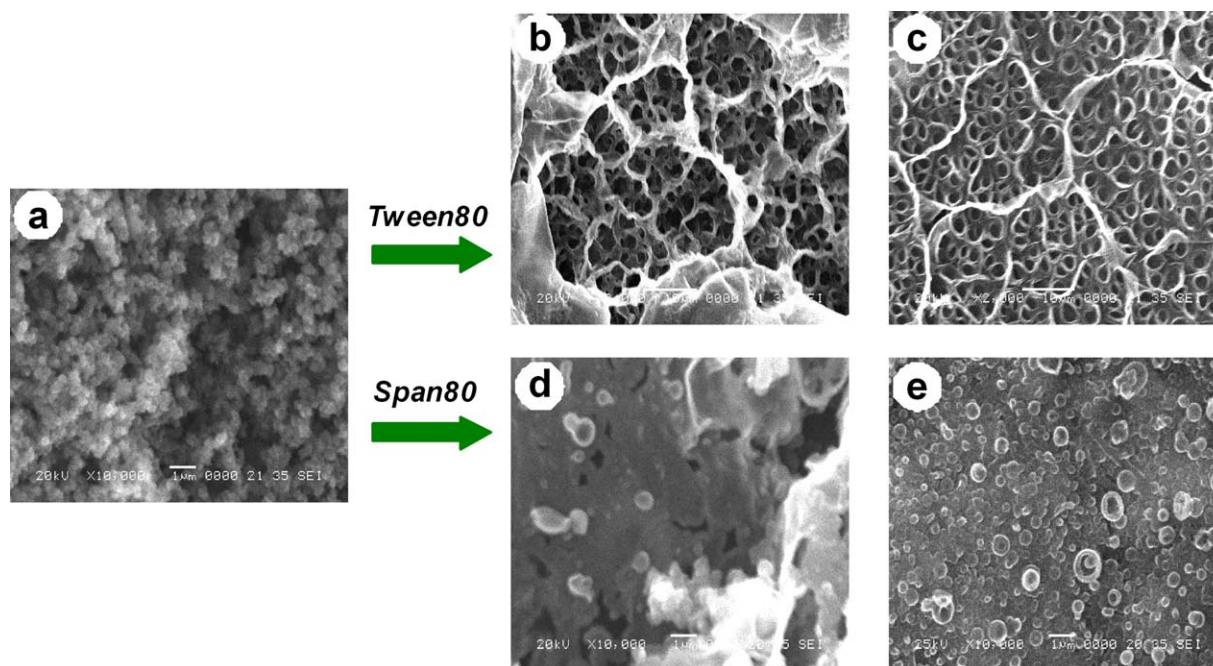
Figure 2. SEM images of PPy films: (a) PPy synthesized without any surfactants at 25°C (R3); (b, c) PPy synthesized with Tween80 as surfactant at 25°C and 0°C, respectively (R5 and R6); (d, e) PPy synthesized with Span80 as surfactant at 25°C and 0°C, respectively (R7 and R8). [Color figure can be viewed in the online issue, which is available at wileyonlinelibrary.com.]
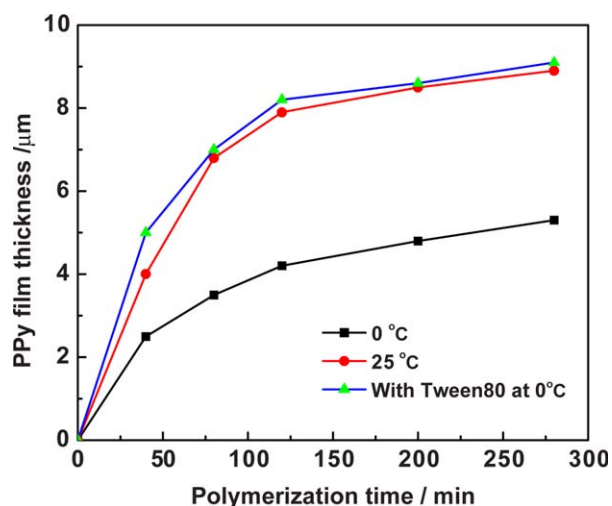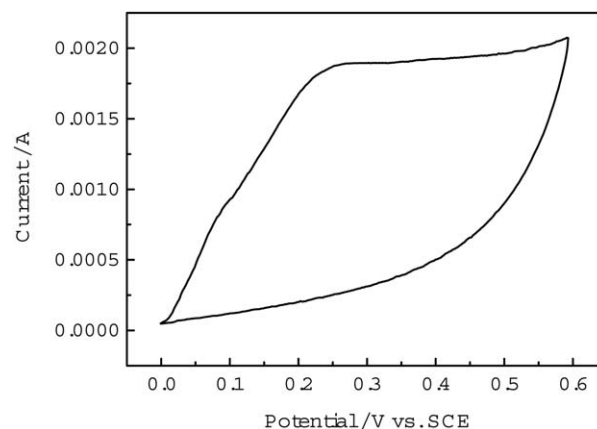
Figure 3. The relationship between PPy film thickness and polymerization time at different reaction temperature with/without surfactant. [Color figure can be viewed in the online issue, which is available at wileyonlinelibrary.com.]

Figure 4. CV curve of the electrode based on synthesized PPy films (R6) in $1M$ NaNO$_3$ with a sweep rate of 25 mV s^{-1} at 25°C.

The effect of polymerization time on PPy film thickness is shown in Figure 3. Clearly, the film thickness gradually increases with polymerization time increasing. Without adding any surfactant, the obtained PPy film at 25°C is much thicker and its thickness increases more quickly with time than the PPy film synthesized at 0°C, revealing that the polymerization rate is low at cooler temperature. The lower polymerization rate benefits the α–α couplings between Py monomers, obtaining PPy with higher conductivity.[29] When adding the surfactant at 0°C, such as Tween80, changing trend of PPy film thickness is similar to the PPy film synthesized at 25°C, which can be attributed to the solubilization caused by the surfactant. That is to say, more Py monomers gather at the oil/water interface under the action of surfactant, resulting in higher growth rate of the PPy film.

Electrochemical Characterization

The electrochemical properties of the synthesized PPy films as electrode materials were studied by CV measurements. The specific capacitances and electric conductivities of PPy films obtained at different conditions can be calculated and measured, shown in Table II. It can be seen that, from this table, sample R6 has the highest specific capacitance of 261 F g^{-1}. This result is connected with the microstructure of R6, and its corresponding CV curve is illustrated in Figure 4. The approximately rectangular shape of CV curve indicates a good pseudo-capacitance performance with symmetrical redox behavior. In comparison with the samples prepared at room temperature, PPy films prepared at 0°C exhibit higher specific capacitance values, which are presented by the data of Table II. This can be attributed to the relatively high conductivity of the PPy, synthe-

sized at low temperature, in the doped state. Besides, at the same polymerization temperature, the obtained PPy with addition of surfactants shows improved specific capacitance and the prepared PPy films with Tween80 as the surfactant have higher specific capacitance that that with Span80 as the surfactant. When adding the surfactants, especially for Tween80, PPy films present highly porous, amorphous morphologies. This means the polymer has large surface area which is beneficial to the ion diffusion and storage within the material, so the sample R6 exhibits the highest specific capacitance.

As is known to all, conducting polymers may occur swelling and shrinking during the intercalating/deintercalating (redox) process, which often lead to mechanical degradation of the electrode based on the conducting polymers and fading its electrochemical performance during cycling. PPy-based electrodes often remarkably degrade under less than a thousand cycles. For example, the PPy electrode with an initial capacitance of 120 F g^{-1} was degraded by 50% in the first 1000 cycles at a constant current density of 2 mA cm^{-2}.[30] The cycling performance of sample R6 was investigated by CV. Figure 5 shows the specific capacitance values of electrodes based on R6 as a function of cycle numbers. Obviously, R6-based electrode has relatively good cycling stability and its capacitance retain about 75% after 1000 cycles. Sample R6 with highly porous structure could effectively reduce cycling degradation problems caused by volumetric changes (swelling and shrinking) during the charging and discharging process, resulting in relatively good electrochemical stability.

CONCLUSIONS

Self-assembled PPy free-standing films have been prepared by oil/water interfacial polymerization in the presence of long-chain surfactants (Tween80 or Span80). The obtained PPy films

Table II. Specific Capacitances of PPy Films Obtained at Different Conditions

Samples	R1	R2	R3	R4	R5	R6	R7	R8
Specific capacitance (F g^{-1})	86	165	78	142	149	261	125	230
Conductivity (S cm^{-1})	1.6	3.8	4.2	8.3	3.5	4.7	3.7	4.5
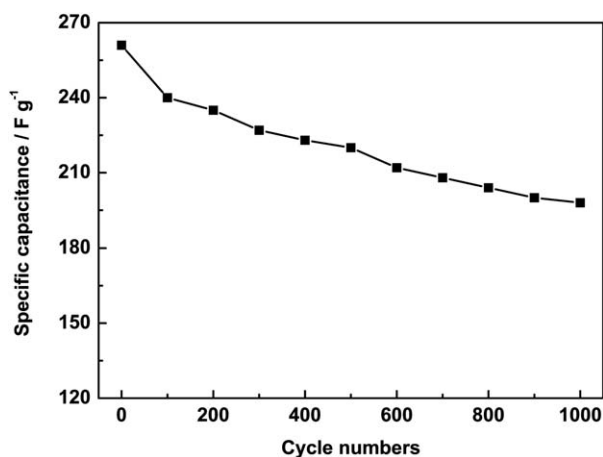
Figure 5. Cycling stability of synthesized PPy films (R6) with cycle numbers from 1 to 1000 in $1M$ NaNO$_3$ at 25 mV s^{-1}.

exhibit highly porous structures with the assistance of Tween80, while they present vesicular structures with the assistance of Span80. Besides, PPy films prepared at low temperature have smaller and more pores or vesicles. These PPy films show higher capacitance than those synthesized by the same method without any surfactants. Especially, the maximum specific capacitance is 261 F g^{-1} at 25 mV s^{-1} for the sample R6, and it displays relatively good electrochemical stability (the retention rate of specific capacitance is 75% after 1000 cycles). Furthermore, the strategy we proposed here provides a facile and effective approach to synthesize PPy films with good electrochemical performance for supercapacitor application.

REFERENCES

1. Huang, J. Y.; Wang, K.; Wei, Z. X. *J. Mater. Chem.* **2010**, *20*, 1117.

2. Wang, J.; Xu, Y. L.; Yan, F.; Zhu, L. B.; Wang, J. P. *J. Power Sources* **2011**, *196*, 2373.

3. Fan, L. Z.; Maier, J. *Electrochem. Commun.* **2006**, *8*, 937.

4. Sadki, S.; Schottland, P.; Brodie, N.; Sabouraud, G. *Chem. Soc. Rev.* **2000**, *29*, 283.

5. Wang, L. X.; Li, X. G.; Yang, Y. L. *React. Funct. Polym.* **2001**, *47*, 125.

6. Chartuprayoon, N.; Hangarter, C. M.; Rheem, Y.; Jung, H.; Myung, N. V. *J. Phys. Chem. C* **2010**, *114*, 11103.

7. Biso, M.; Ansaldo, A.; Picardo, E.; Ricci, D. *Carbon* **2012**, *50*, 4506.

8. Lee, T. W. *Adv. Funct. Mater.* **2007**, *17*, 3128.

9. Yeganeh, M.; Saremi, M.; Rezaeyan, H. *Prog. Org. Coat.* **2014**, *77*, 1428.

10. Wang, C.; Zheng, W.; Yue, Z.; Too, C. O.; Wallace, G. G. *Adv. Mater.* **2011**, *23*, 3580.

11. Snook, G. A.; Kao, P.; Best, A. S. *J. Power Sources* **2011**, *196*, 1.

12. Sun, W.; Chen, X. *J. Power Sources* **2009**, *193*, 924.

13. Yue, B.; Wang, C.; Wagner, P.; Yang, Y.; Ding, X.; Officer, D. L.; Wallace, G. G. *Synth. Met.* **2012**, *162*, 2216.

14. Wang, G.; Zhang, L.; Zhang, J. *Chem. Soc. Rev.* **2012**, *41*, 797.

15. Mallouki, M.; Tran-Van, F.; Sarrazin, C.; Chevrot, C.; Fauvarque, J. F. *Electrochim. Acta* **2009**, *54*, 2992.

16. Huang, J.; Kaner, R. B. *Chem. Commun.* **2006**, 367.

17. Li, R.; Chen, Z.; Li, J.; Zhang, C.; Guo, Q. *Synth. Met.* **2013**, *171*, 39.

18. Georgakilas, V.; Dallas, P.; Niarchos, D.; Boukos, N.; Trapalis, C. *Synth. Met.* **2009**, *159*, 632.

19. Dallas, P.; Niarchos, D.; Vrbanic, D.; Boukos, N.; Pejovnik, S.; Trapalis, C.; Petridis, D. *Polymer* **2007**, *48*, 2007.

20. Bora, C.; Dolui, S. K. *Polymer* **2012**, *53*, 923.

21. Liu, P.; Wang, X.; Li, H. *Synth. Met.* **2013**, *181*, 72.

22. Hou, L.; Yuan, C.; Li, D.; Yang, L.; Shen, L.; Zhang, F.; Zhang, X. *Electrochim. Acta* **2011**, *56*, 6049.

23. Han, Y.; Shen, M.; Lin, X.; Ding, B.; Zhang, L.; Tong, H.; Zhang, X. *Synth. Met.* **2012**, *162*, 753.

24. Jin, Y.; Huang, S.; Zhang, M.; Jia, M. *Synth. Met.* **2013**, *168*, 58.

25. Noh, K. A.; Kim, D. W.; Jin, C. S.; Shin, K. H.; Kim, J. H.; Ko, J. M. *J. Power Sources* **2003**, *124*, 593.

26. Liu, J.; Wan, M. X. *J. Mater. Chem.* **2011**, *11*, 404.

27. Shen, M.; Han, Y.; Lin, X.; Ding, B.; Zhang, L.; Zhang, X. *J. Appl. Polym. Sci.* **2013**, *127*, 2938.

28. Maity, A.; Sinha, R. S. *Macromol. Rapid Commun.* **2008**, *29*, 1582.

29. Li, X. G.; Hou, Z. Z.; Huang, M. R. *J. Phys. Chem. C* **2009**, *113*, 21586.

30. Sharma, R. K.; Rastogi, A. C.; Desu, S. B. *Electrochim. Acta* **2008**, *53*, 7690.